

INTERNAL REPORT SDL-87-05

## TEMPERATURE MEASUREMENTS IN SHOCKED LIQUIDS

Rick Gustavsen

May 1987

Shock Dynamics Laboratory

Department of Physics

Washington State University

Pullman, WA 99164-2814

## TEMPERATURE MEASUREMENTS IN SHOCKED LIQUIDS

Rick Gustavsen  
Shock Dynamics Lab  
Washington State University

### ABSTRACT

Temperature measurement in a shock compressed material is an important, though little developed, area of research. Temperature, when coupled with existing experimental data, can provide a complete (P,V,T) equation of state. For our study, we chose to work with liquids because many of the problems that arise in studying solids can be avoided. In this paper we discuss results of heat conduction calculations and experiments for two experimental geometries: metal foils  $\approx 10\mu m$  thick suspended directly in the liquid, and thin ( $\approx .2\mu m$ ) metal films deposited on a fused silica substrate and in contact with the liquid. Calculations and experiments showed that the  $10\mu m$  foils would not heat up. Our calculations predicted that the  $.2\mu m$  metal films would heat up to  $\approx 30\%$  of the liquid temperature, however, even after a considerable experimental effort, we could not make films this thin survive shock loading.

# TEMPERATURE MEASUREMENTS IN SHOCKED LIQUIDS

## Introduction

Without a knowledge of the temperature or entropy any equation of state which is developed for a shocked material will be incomplete. From what are now routine shock wave experiments the state of stress, the particle velocity, and the shock velocity can be measured. Using the shock jump conditions the energy  $E$  and the volume  $V$  can be calculated to give an  $E(P,V)$  equation of state. Successful measurements of the temperature taken with existing shock wave data would provide complete thermodynamic information.

For the modest temperature changes of condensed materials at shock strengths of 1 - 100 Kbar optical emission methods are not feasible. Rosenberg and Partom (1981, 1984) have attempted measurements using metal thermistors in polymethylmethacrylate, a polymer, while Bloomquist and Sheffield (1980) have used thermocouples in shock compressed solids. Our approach was to monitor the thermal resistivity of thin metal foils/films in contact with shocked liquids.

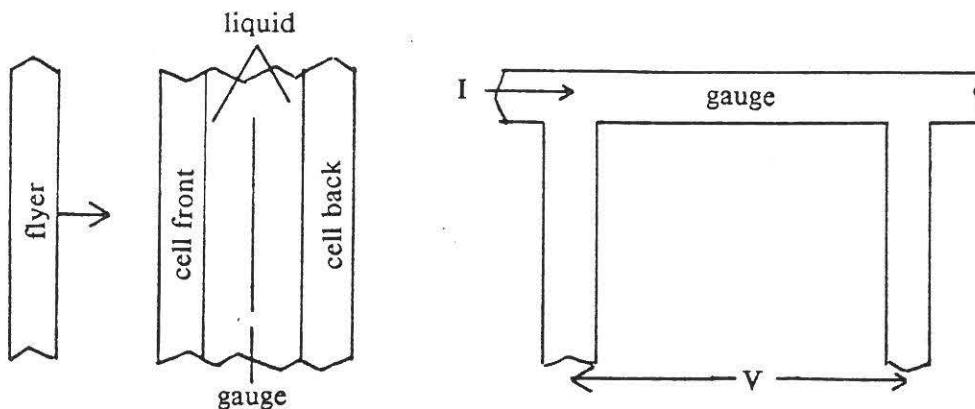
There are good reasons for studying liquids rather than solids. First, liquids undergo large temperature changes at modest shock strengths. Second, the liquid can contact the gauge directly, rather than through a layer of bonding material. Third there will be no strength effects since the gauge is loaded hydrostatically. Finally the temperature throughout the liquid will be homogeneous.

It is important to remember that temperature measurements require time for the probe to reach thermal equilibrium with the sample. In shock wave experiments the time scale is only  $1\mu s$  so the probe won't have time to reach the temperature of the sample.

Secondly, we always measure some property of the probe, and not the temperature. For shock wave experiments in which we monitor a resistance change, this change can come from a number of sources. These are; gauge deformation, pressure effects (piezoresistance) and temperature effects (thermoreistance). To optimize our experiments for temperature effects we used an experimental geometry which minimized gauge deformation, and a gauge material with a high ratio of thermoresistance to piezoresistance. Much of the guage material ground-work was done by S. Tolczynski (1983?)

### Suspended Foils

Perhaps the most obvious experimental scheme is to suspend a metal foil in the liquid and measure its resistance change as the shock passes. This basic concept is illustrated below.



In order to understand the resistance change of the gauge it is necessary to know the pressure and temperature in the gauge. The pressure is calculated using the impact velocity, the Hugoniot of the liquid, flyer, and other cell materials, and normal shock wave techniques. The temperature is estimated from the liquid EOS (assumed correct) and a solution of the heat conduction equation;

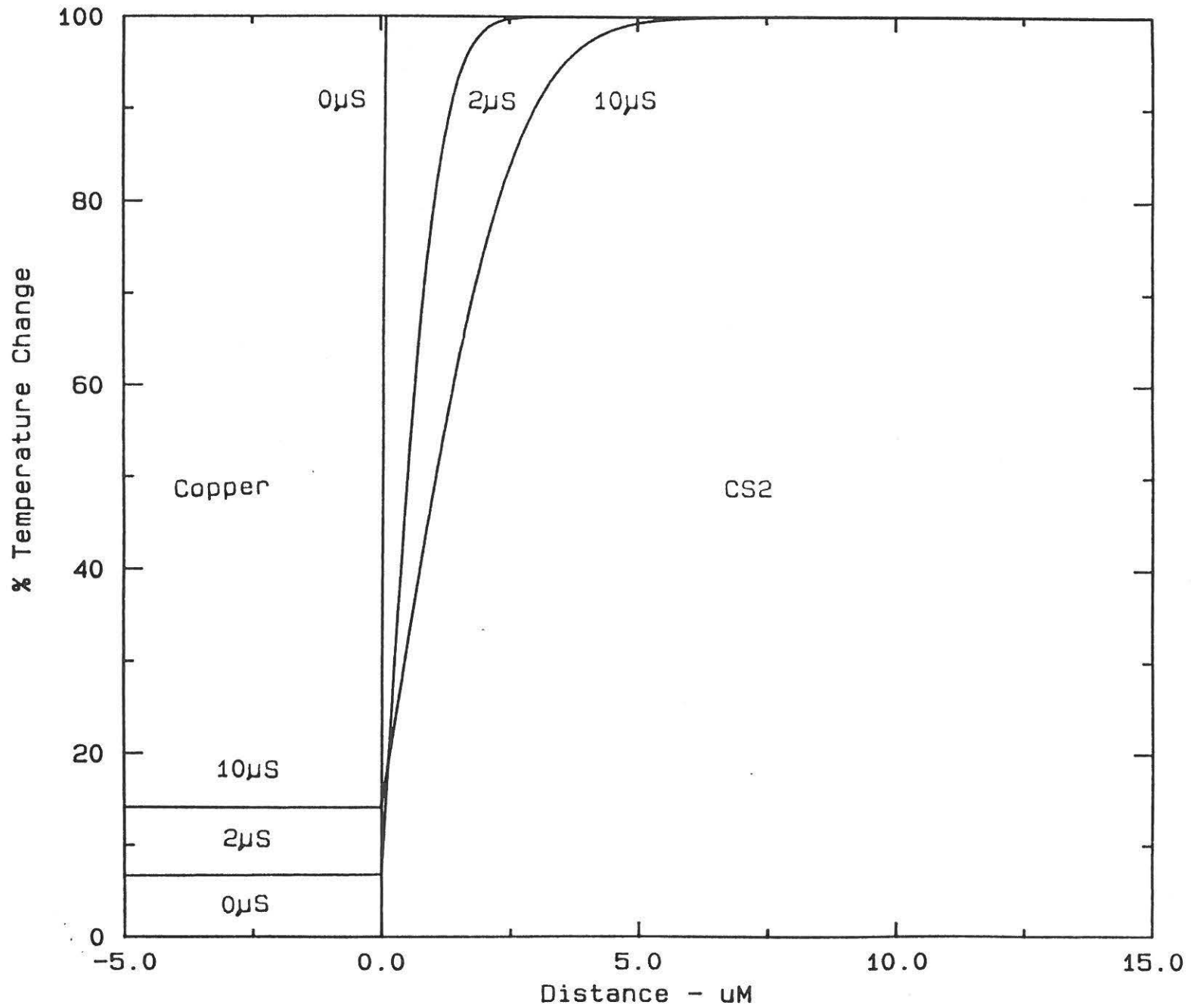
$$C \rho \frac{\partial T}{\partial t} = K \frac{\partial^2 T}{\partial x^2} ,$$

Where  $C$  is the specific heat,  $\rho$  is the density, and  $K$  the thermal conductivity.

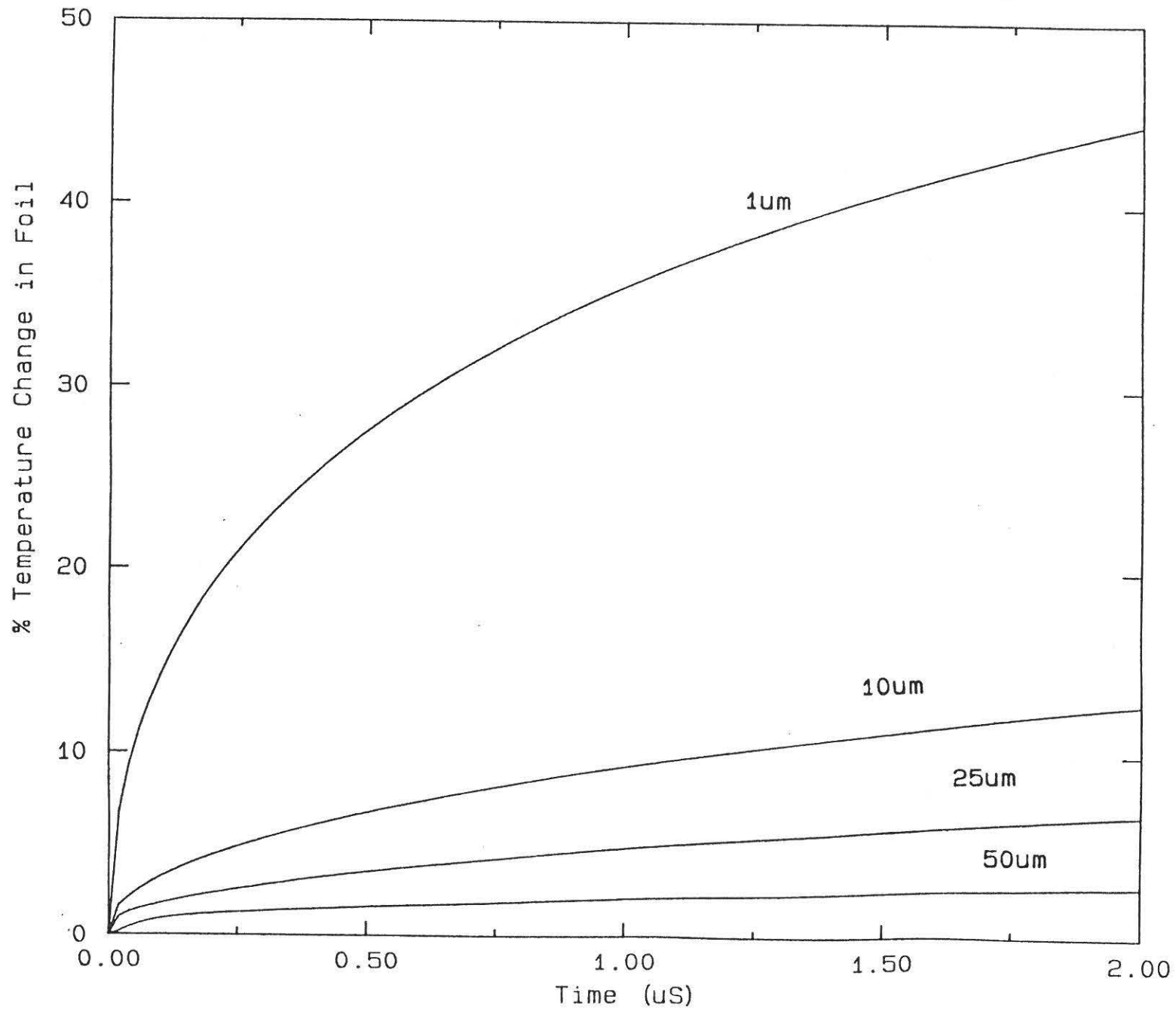
For this experimental geometry I found a closed form solution which appears in Appendix I. Because of previous experimental and theoretical work in our lab  $CS_2$  was chosen as the liquid. Copper was picked as the gauge material. The following graphs show the results of the heat conduction calculations for these materials.

- (1) Space temperature profiles of a  $10\mu m$  copper foil in  $CS_2$ . The Copper gauge extends from  $-5\mu m$  (gauge center) to 0. The  $CS_2$  extends from 0 to  $\infty$ . Note that the copper foil is actually cooling the  $CS_2$ .
- (2) Equilibration time depends strongly on foil thickness. Foils of 1 -  $2\mu m$  thickness show significant equilibration while foils greater than  $10\mu m$  thick show very little equilibration. Temperature is for the foil center.
- (3) Equilibration time depends strongly on the thermal conductivity of the liquid. For a  $10\mu m$  copper foil in liquid  $CS_2$  we see that  $K_o$ , the ambient  $CS_2$  thermal conductivity, must be increased by a factor of 100 or more for significant equilibration.

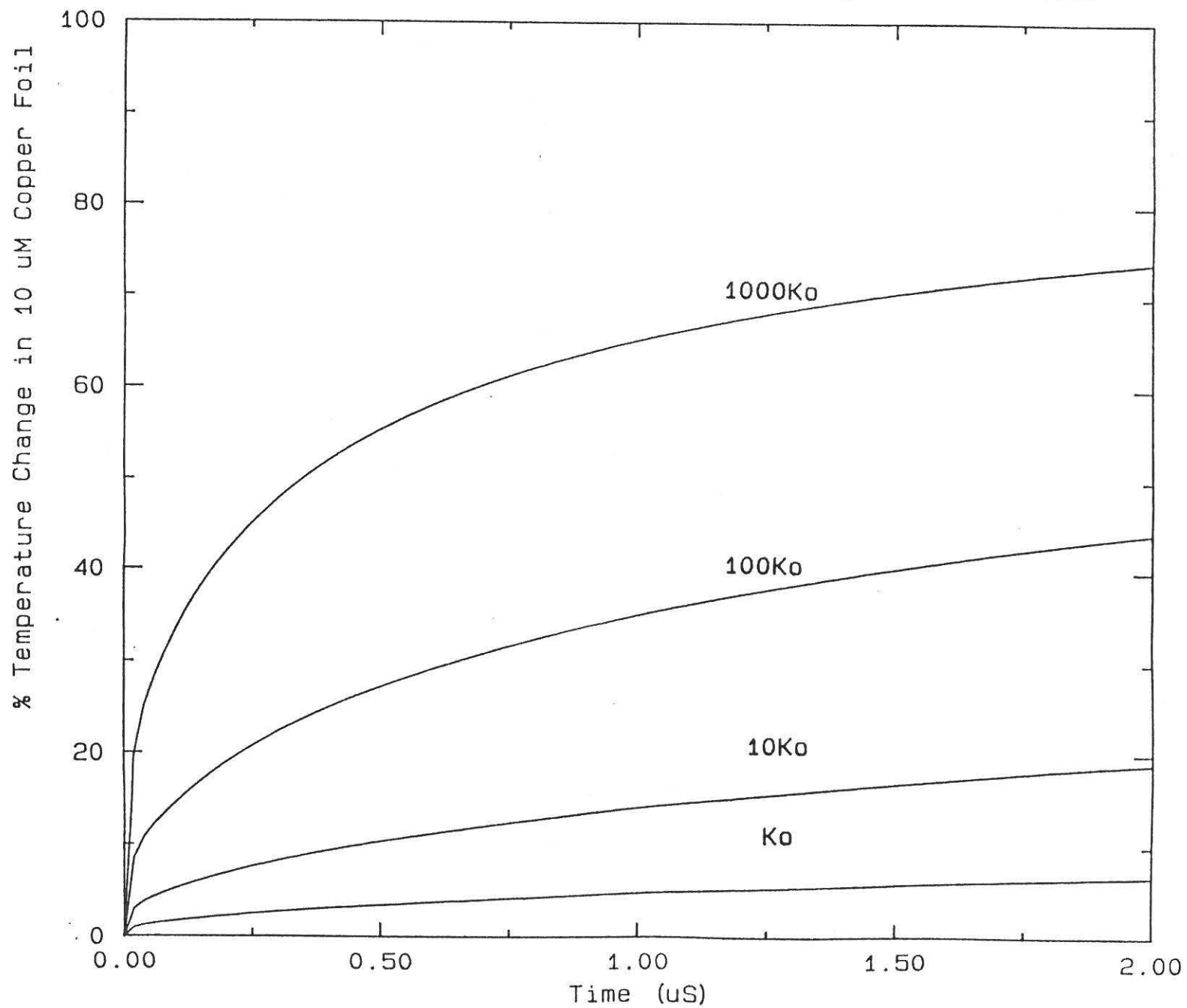
Space - Temperature Profiles of Cu Foils in CS2



Effect of Foil Thickness for Cu Foil in CS2



Effect of Liquid Thermal Conductivity (CS2 as basis)

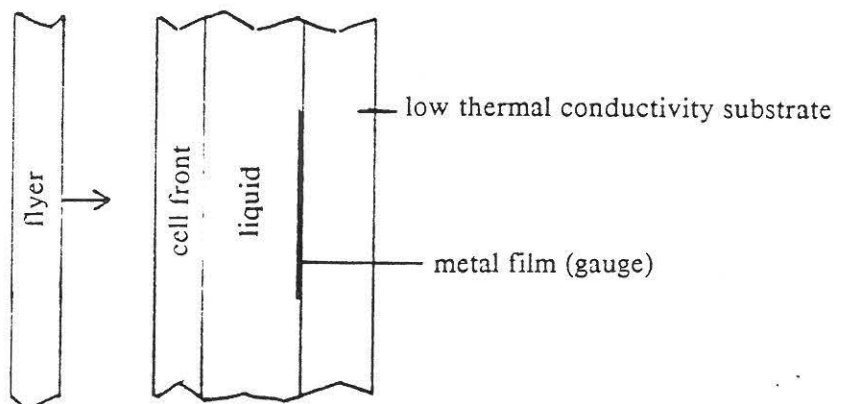


From these studies we conclude that foils of reasonable thickness will not heat up significantly on the one microsecond time scale of shock experiments. (Foils thinner than  $12\mu m$  or .0005" are not available and further would be very hard to work with). To conclude this part of the study two experiments were performed where copper foils  $25\mu m$  (.0010") thick were suspended in cells of liquid  $CS_2$  and shocked to 40 Kbar. Although the liquid reached a temperature of more than 600 K, little resistance change was seen, as predicted by the calculations.

#### Thin Film on a Substrate

For the suspended foils it was impossible to get adequate equilibration without either a very high liquid thermal conductivity or a very thin foil. Since no liquids except mercury have thermal conductivities on the same order of magnitude as metals, and since foils on the order of  $1\mu m$  thickness are too delicate to work with, a new experimental concept was needed.

The primary consideration for the new experimental design was that it use a very thin metal gauge layer. Our basic idea was to deposit a very thin metal film ( $\approx .2\mu m$ ) on a substrate that has low thermal conductivity, and is elastic in the pressure range of interest. The gauge film is thus in thermal contact with the liquid on one side and the substrate on the other. The experimental geometry is illustrated below.



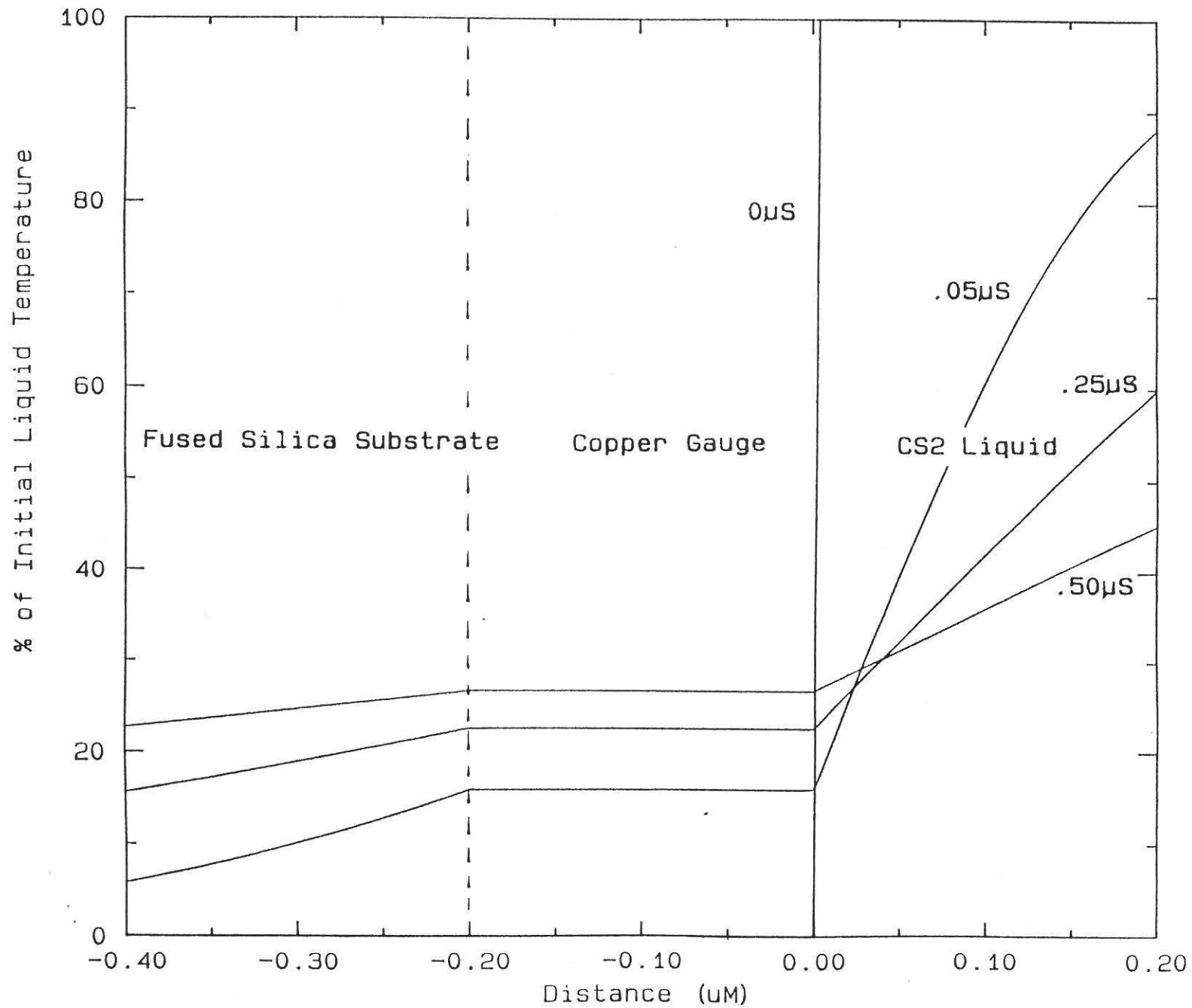
The first task was to solve the heat conduction equation for this geometry. Appendix II outlines the solution and gives a closed form result. The second task was material selection. Fused silica was chosen as the substrate material since it has a thermal conductivity on the same order as liquids (see AIP handbook) and is elastic to about 90 Kbar (see Barker and Hollenback, 1970). As in the suspended foil experiments, the liquid would be  $CS_2$ , and initially the film would be copper. For these materials solution of the heat conduction equation showed the following;

- (4) Space temperature profiles show that the liquid is cooled by the film and substrate, but that there is substantial heating of the film.
- (5) Effect of film thickness; These calculations show that films on the order of  $.15 - .35\mu m$  will have relatively quick equilibration times while thicker films will heat up more slowly.

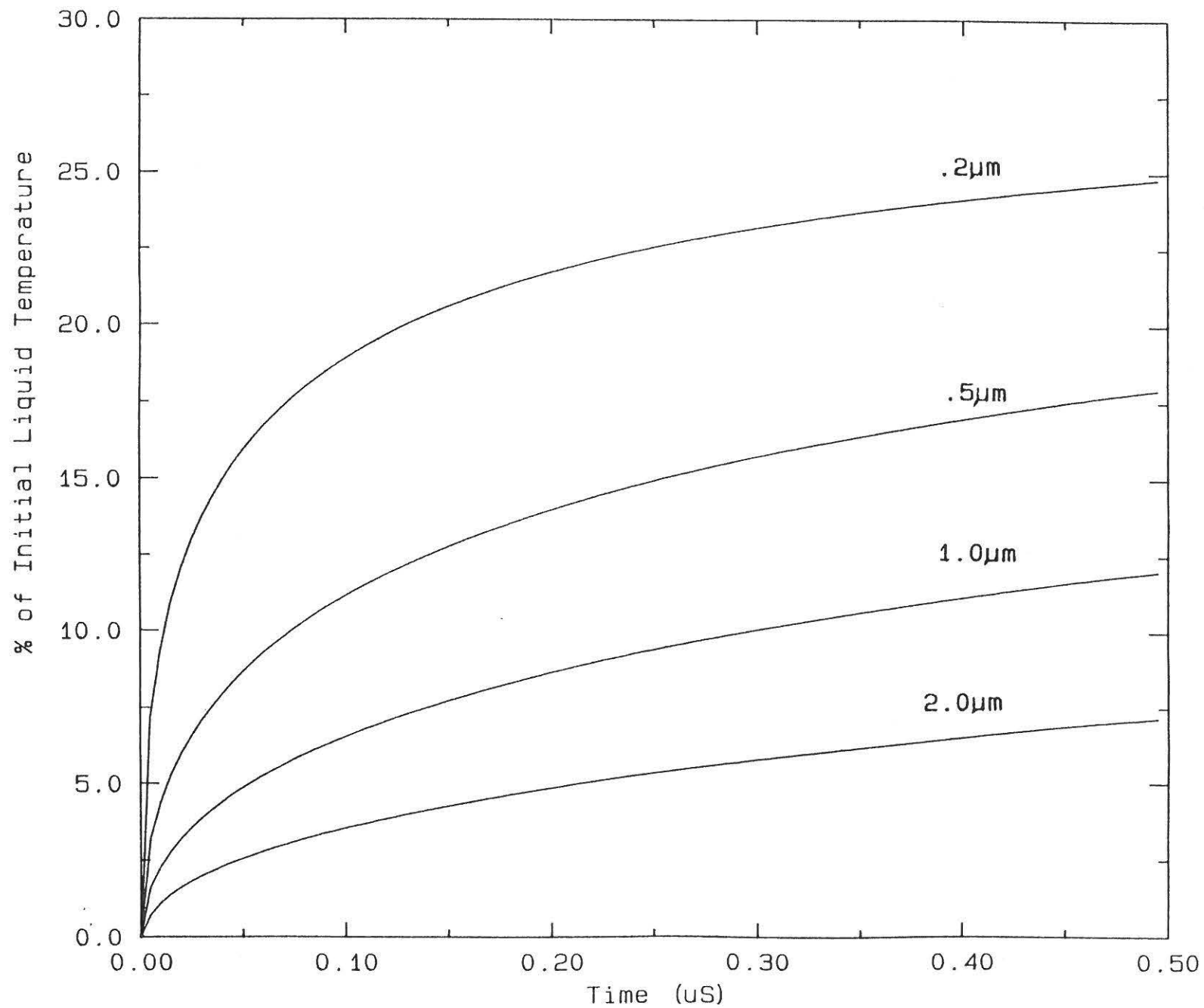
#### Film on Substrate Experiments

Because of the favourable predictions of our heat conduction calculations we thought it would be worthwhile to try some experiments. A large number of experiments were performed over an extended period of time. In order to avoid rambling, I have tried to do as much condensing in this section as possible. The experiments can be divided into two parts. The division is in terms of the goals of the experiments, and coincidentally, it is also chronological. In the first part the objectives were to find a gauge material, a process for putting it on the substrate, and techniques for characterizing it. The objectives of the second part were simple: find why the gauges were not surviving.

Space Temperature Profiles for Fused Silica/.2 $\mu$ M Cu film/CS2

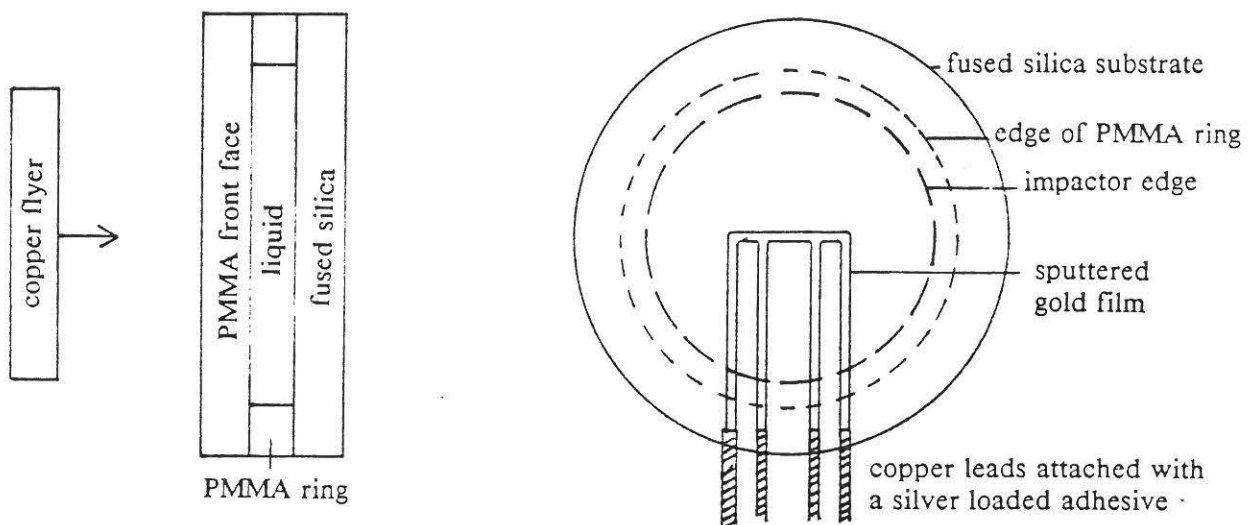


Effect of Film Thickness on Equilibration Time (Fused Sil/Cu/CS<sub>2</sub>)



I started playing the gauge material and process game rather naively. In our lab we had been using copper as a plating material for trigger and tilt contacts. I had done all the initial heat conduction calculations with copper. It therefore seemed most natural that I should try to make gauges of vapor deposited copper. Several gauge ideas were tried, all having the common feature of being four lead resistance gauges. The differences were all in how the thick copper leads, which carry signals to and from the outside world, were attached to the vapor deposited leads and active element. The ideas tried included plating over thick leads epoxied in the fused silica, pasting thick leads onto the vapor deposited leads using silver loaded cement, and plating directly over copper posts stuck through the fused silica substrate. In experiments none of these survived long enough to give data. At this time we attributed the breakage to either poor ductility or poor adherence of the copper films.

The next gauge material was gold, which was sputtered at 8 KV in a 30 millitorr argon atmosphere. Gold is a very ductile material and I felt that the leads would be more likely to stretch than to break. The sputtering process gave films which sometimes had good adherence, although it was just often bad. (Adherence is measured by the tape test, see Appendix IV). The experimental assembly for the sputtered gold film experiments is shown below.



This basic experimental geometry was used for most of the experiments which followed. Three experiments were performed using sputtered gold films. In all three the gauges appeared to last longer than  $.2\mu s$ . The only difference between shots was in pressure. In the third shot a much improved recording system was used. This recording system gave a much cleaner signal, faster rise time etc, and was used with only slight modification on subsequent shots (See Appendix V for details).

While the gauges made by sputtering gold on fused silica substrates appeared to survive, their output did not match well with theory. We had not, however, characterized the gauges very well, but had assumed that the gold film had the properties of the bulk. To characterize the gauges we measured their thickness using a simple interference technique. The details of this technique are presented in Appendix III. We next measured the resistance, and since we now knew the dimensions, we could calculate the resistivity. The bulk resistivity of the sputtered films was always higher than that of the bulk. Finally, we constructed a very simple system for measuring the resistance - temperature properties of the film.

The resistance - temperature properties of the films were not what I had naively expected. The first time the gold film was heated its resistance did not increase linearly with the temperature. When cooled the resistance decreased almost linearly to a room temperature value much lower than the initial resistance. After about three to four cycles the R-T properties of the film had stabilized.  $R(0^{\circ}C)$  was stable and the resistance increased linearly with temperature. The appropriate coefficients were also near their bulk values. Belser and Hicklin (1959) did a study in which metal films showed similar behavior on temperature cycling. This confirmed our belief that the gauges were being annealed in the temperature cycling process.

Since it seemed the temperature cycling process was annealing the films we decided to anneal them first. After annealing at  $300^{\circ}C$  in air or vacuum the resistivity and the temperature

coefficient of resistivity were that of bulk gold. The resistance - temperature properties were also highly repeatable on cycling. The films themselves, however, had become soft and poorly adhering. In an effort to improve adherence many substrate cleaning techniques were tried. Appendix IV lists the best one. It was found, however, that no process would make gold, especially after annealing, stick to a fused silica substrate. Gold films are inherently soft and poorly adhering (Archibald and Parent, 1975). Two experiments were built using the annealed gold films. One was not fired because the gauge peeled off when the cell was filled. The other gauge broke as soon as the shock wave passed the gauge plane.

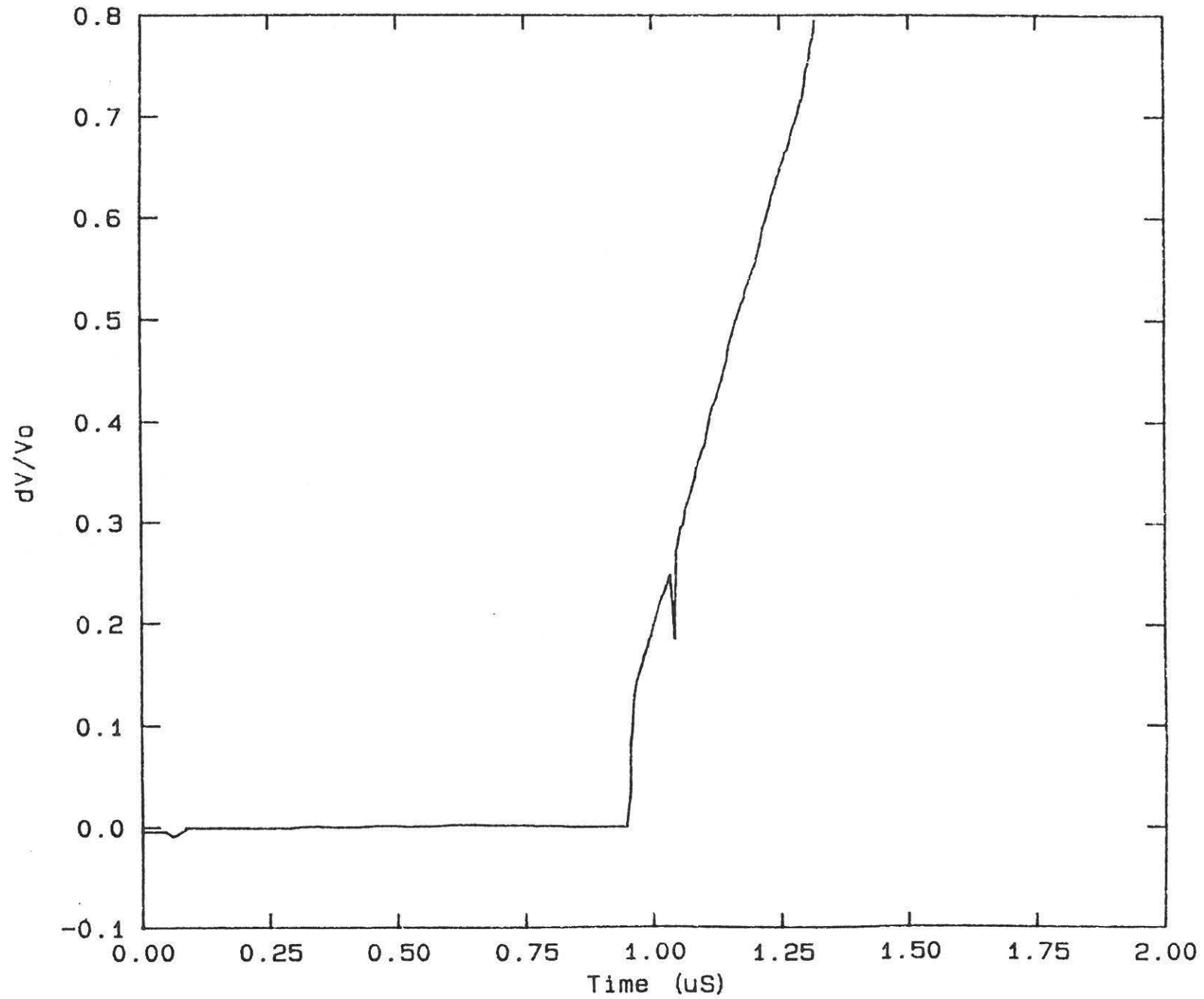
After some reading and a little personal experimenting, I decided to try making the gauges from aluminum vapor deposited off tungsten helices. Aluminum has the following advantages: First, it adheres to  $SiO_2$  quite well. Second, I found that even before annealing its resistance - temperature properties were quite linear and repeatable. After annealing at  $300^\circ C$  in vacuum the resistance - temperature properties and resistivity were those of bulk aluminum. In addition, the aluminum films actually adhered better after annealing. Finally, aluminum thin films are used as conductors in integrated circuit devices because of their good electrical properties and good adherence to silicon and its oxides. (For a reference see Muller and Kamins, p. 48 and 49). The only drawback of using aluminum is that it is hard to solder. I generally used a silver loaded paint or epoxy to make connections between the copper leads and the vapor deposited gauge.

With all the good news, about aluminum films I hurriedly built an experiment. Although the experimental geometry was the same as the "successful" gold film shots, the aluminum gauge broke as soon as the shock wave crossed its plane. Thinking perhaps I had made some blunder I repeated the shot, but with the same result. I next assumed there was a problem with the experimental geometry. I built three shots in which the liquid layer and PPMA ring were removed, and the PMMA front face was epoxied directly onto the substrate/gauge surface.

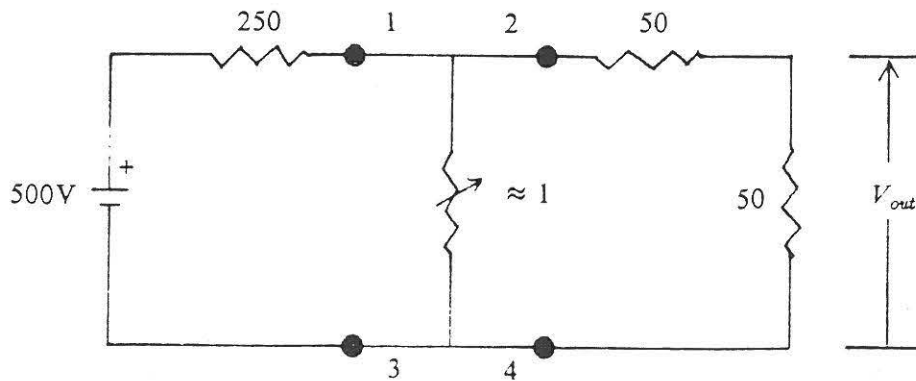
Impactors of differing sizes and shapes were used, this being the experimental geometry variable. In all three experiments the gauges lasted more than half a microsecond after shock arrival. Since the experiments were entirely to find which geometry worked best, little characterization and no post shot analysis was done on these experiments. In the end they really only tell us that a gauge will survive if it has a uniform solid epoxied to its surface.

The experimental geometry which worked best for the "PMMA" shots was little different than that used on all the previous shots. Nevertheless, I went ahead and built another liquid cell shot which, of course, failed. Following this, I built several more experiments in which the vapor deposited area outside the active element was thickened with various materials, which were vapor deposited over the aluminum. All these shots failed. Because of the unexpected failures the experiments I performed during this time period lacked goals and direction. It was a game of try this and try that and hope something works. All of these shots did, however, produce a characteristic record similar to that seen in figure 6. The large fast rising voltage was attributed to stretching or breaking of the gauge leads by Dr. Y.M. Gupta and myself. Possible reasons for lead breakage were thought to be; gauge too thin, gauge not adhering well, gauge too brittle, impact geometry, or a possible reaction of the liquid with the gauge.

A Typical Large, Fast Rising Voltage



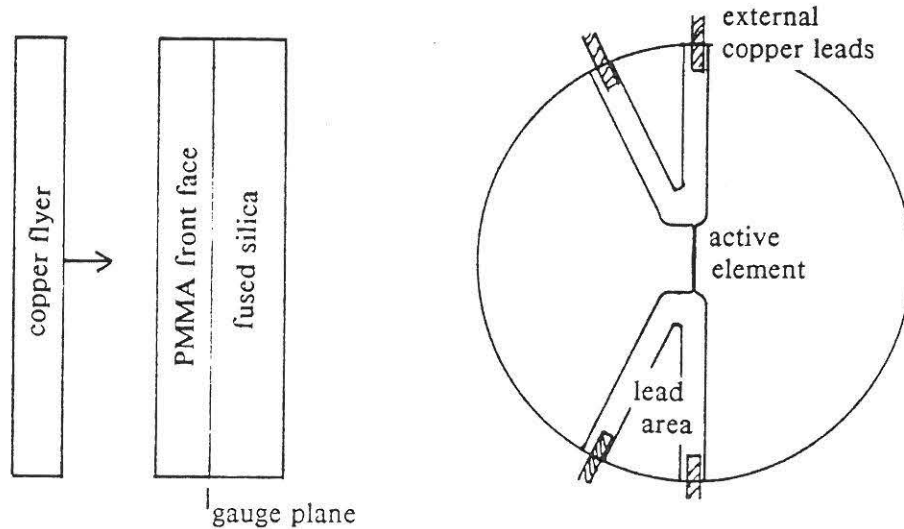
A discussion with Dr. G.E. Duvall concerning the large fast rising voltage, in the context of the equivalent recording circuit shown below,



led us to believe that the large fast rising voltage could only be caused by breakage of the active element. It could not be caused by breakage of the leads labeled 1,2,3 or 4. While our analysis turned out to be incorrect, (it is possible to dump the charge on the cables through the scope resistor in the event of lead breakage), the meeting itself produced two positive goals.

Our first goal was to build a circuit whose output would give a different signature voltage for different leads or combinations of leads breaking. This might provide a clue as to the source of the large fast rising voltage. This circuit along with its signature voltages is shown in the last part of Appendix V. The second goal was to use this circuit as a tool in a series of experiments designed to determine where and or why the gauges were breaking. Also a more careful characterization and analysis was to be done.

The first three experiments using the "lead breakage circuit" were built with PMMA front faces epoxied directly to the gauge/substrate as shown below.



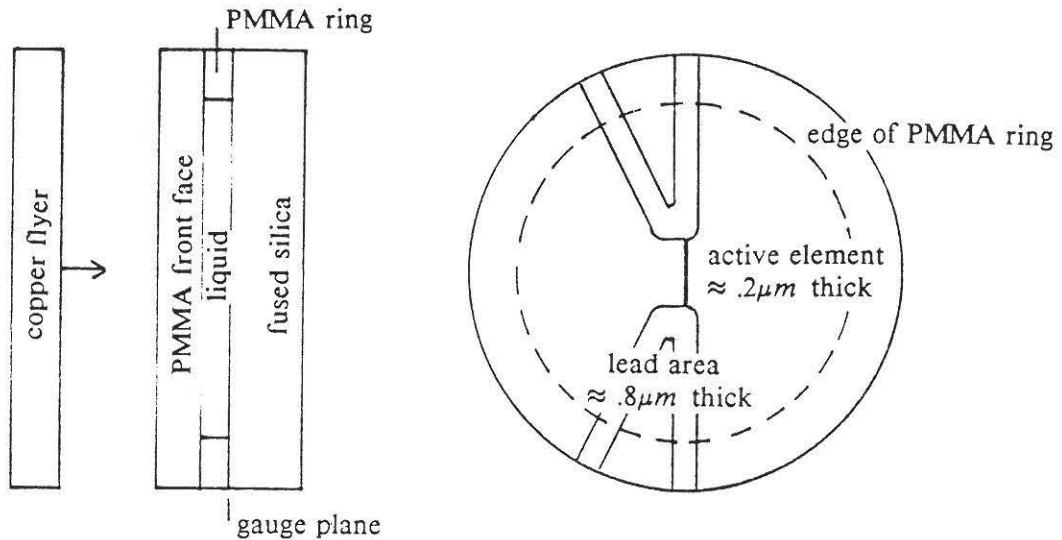
Since shots like this had worked in the past we felt that by doing a careful preparation and analysis these shots could be used as a benchmark for comparison. The results from three identical experiments follow.

- (1) With a PMMA front face attached directly to the gauge/substrate the gauge will last more than  $.5\mu s$ .
- (2) The gauge broke in the lead area, all four leads breaking simultaneously. Breakup time tended to coincide with the arrival of compression or relief waves.
- (3) The resistance change of the gauge could be described by

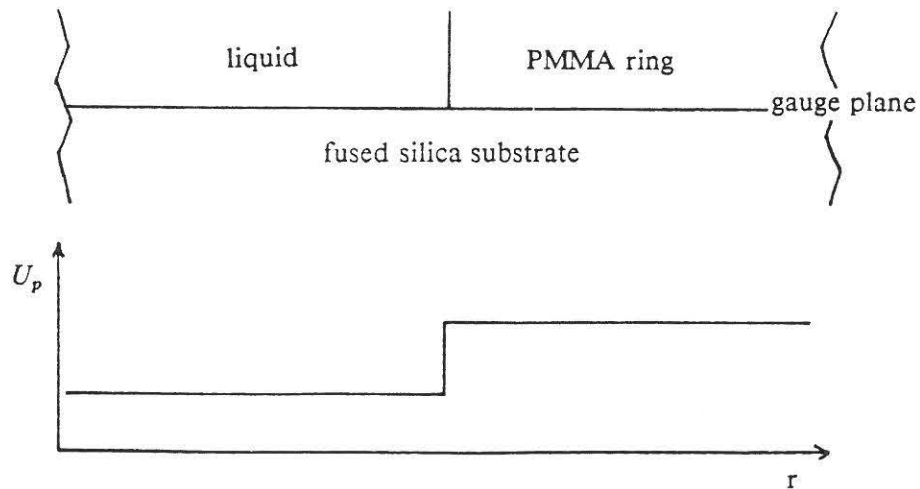
$$\frac{\Delta R}{R_0} = \alpha T + \beta P$$

where  $\alpha$  is the measured temperature coefficient of resistivity,  $T$  is the mean of the temperatures of the PMMA and fused silica, as calculated by the shock up program,  $P$  is the shock pressure, and  $\beta P$  the fractional change in resistance as measured by Bridgman. (Vol 7, p. 169-221)

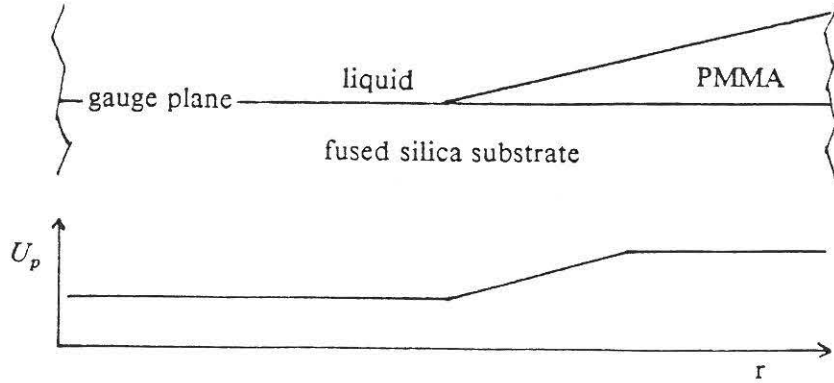
The next two experiments were perhaps the most important in figuring out why the gauges were breaking. They both were liquid cells, containing water. (We thought that water, being quite inert, wouldn't react with the aluminum gauge. The first water experiment was constructed similar to all the other liquid cell shots. Its schematic is shown below.



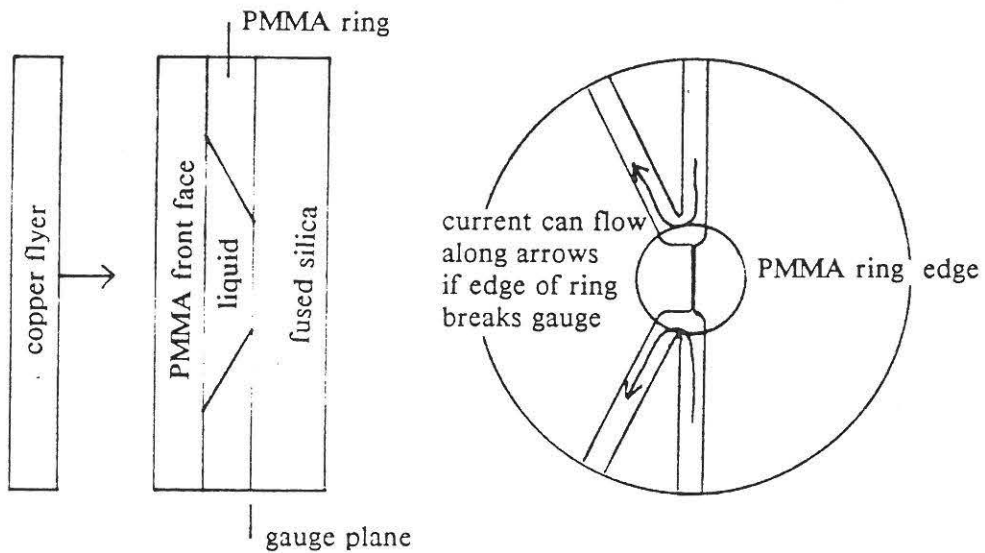
Analysis of the output from the "lead breakage circuit" showed that all four leads broke at the time the shock passed the gauge plane. We suspected that the gauge leads were being cut off by the inside edge of the PMMA ring. The next experiment was designed primarily to see if the rings' cutting action could be minimized. For the typical liquid cell there would be a sharp velocity gradient produced by an edge.



In order to minimize this effect we designed a tapered ring which we hoped would produce a particle velocity pattern more like that shown below.



In addition to the ring being tapered, the edge of the PMMA ring contacted the gauge/fused silica surface at a location such that if it were to cut the gauge, a signal different from the 4 leads breakage value would be recorded. The shot geometry and the location of the ring edge are shown below.



Analysis of the records from this experiment indicate that at the time the shock wave passed the gauge plane the gauge broke along the edge of the PMMA ring. Combining the result of this experiment with the previous one strongly suggested that the gauge was being cut by the PMMA ring. Implicit is that a vapor deposited gauge lead of  $.5 - 1\mu m$  thickness cannot withstand the cutting of an edge of PMMA. Two obvious ways to avoid this problem are to thicken the gauge in the lead area, or to avoid the PMMA ring and its cutting edge altogether. One experiment was done in which the lead area was thickened to about  $15\mu m$  using a silver thick film material. The gauge broke in the active area. This was either because the active area was too thin, or possibly because of the step from  $15\mu m$  to  $.2\mu m$ .

In each of the last three experiments the fused silica disk on which the gauge was deposited was held only by its sides. This eliminated the possibility of a ring edge cutting the leads. In all three experiments the leads were made between  $1.5$  and  $2.0\mu m$  thick. Active elements were  $.18$ ,  $.21$ , and  $.50\mu m$  thick. In all three experiments the leads survived at least  $3\mu s$ . The active elements, however, all broke upon shock arrival. The leads surviving, taken with the active element breaking suggests that gauge thickness is also very important to gauge survival in liquids. Perhaps it is as important as eliminating the cutting edge of the PMMA ring.

### Conclusion

While we have not been successful in producing a temperature measurement, we have made progress on the following points. First, solution of the heat conduction equation and preliminary experiments show that very thin ( $\approx 1\mu m$ ) metal films must be used for thermoresistance gauges. For a copper foil of  $1.0\mu m$  or greater thickness to heat up substantially, it must be surrounded by a material of high thermal conductivity. Second, for survival of thin metal films on fused silica substrates, survival of the film is the major unsolved experimental problem.

If the films would survive much experimental and theoretical work would be needed to ensure that the measured resistance change corresponded to a temperature change. Further work would be needed to calculate the liquid temperature.

Regarding gauge survival our work leads us to the following conclusions; In order for the gauge to survive we must first eliminate the edge of the PMMA ring which has been shown to cut the gauge. Secondly, it seems we need a gauge which is 1.2 - 1.5 $\mu$ m thick. Unfortunately, the sensitivity of a gauge this thick would be too low to provide useful data. The increase in resistance due to temperature would be small with a slow rise time and the decrease in resistance due to pressure would be of the same order of magnitude.

## References

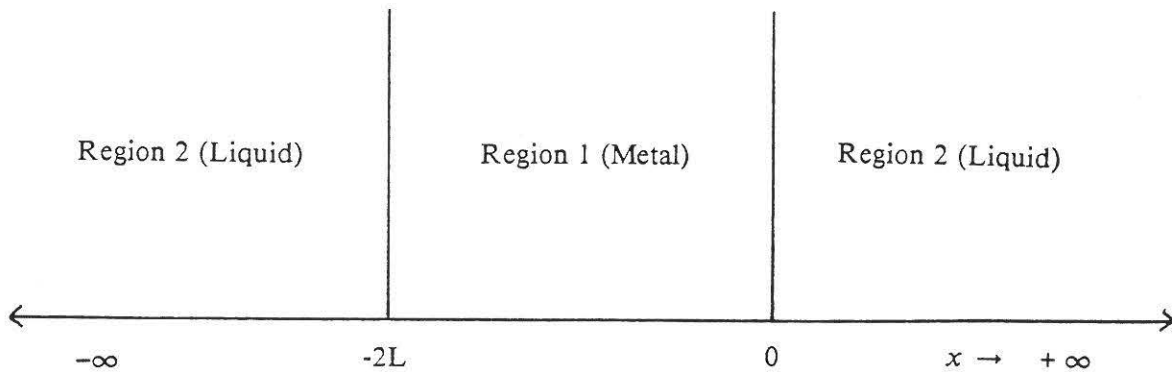
- P. Archibald and E. Parent, *Source Evaporant Systems for Thermal Evaporation*, Presented at the Society of Vacuum Coaters, 4/18/75. Also in *Solid State Technology*, July 1976.
- N.W. Ashcroft and N.D. Mermin, *Solid State Physics*, Holt, Rinehart and Winston, (1976). This book contains many useful tables of properties of materials.
- L.M. Barker and R.E. Hollenbach, *Shock Wave Studies of PMMA, Fused Silica, and Sapphire*, *J. Appl. Phys.* Vol. 41, No. 10 4208 (1970).
- R.B. Belser and W.H. Hicklin, *Temperature Coefficients of Resistance of Metallic Films in the Temperature Range 25 to 600C*, *J. Appl. Phys.* Vol. 30, No. 3, 313, (1959).
- M. Born and E. Wolf, *Principles of Optics*, 3rd Ed., Pergamon Press, (1965)
- D.D. Bloomquist and S.A. Sheffield, *Thermocouple Temperature Measurements in Shock Compressed Solids*, *J. Appl. Phys.* Vol. 51, No. 10, (1980)
- P.W. Bridgman, *The Thermal Conductivity of Liquids under Pressure*, *Collected Experimental Papers*, Vol. 3, p. 158+, Harvard University Press, (1964)
- P.W. Bridgman, *The Resistance of 72 Elements, Alloys, and Compounds to 100,000Kg/cm<sup>2</sup>*, *Collected Experimental Papers*, Vol. 7, p. 169-221, Harvard University Press, (1964)
- H.S. Carslaw and J.C. Jaeger, *The Conduction of Heat in Solids*, 2nd Ed., Clarendon Press, Oxford, (1986)
- D.E. Gray coordinating editor, *American Institute of Physics Handbook*, McGraw Hill, (1964). Section 4 contains the thermal conductivity and other thermal data.
- O.S. Heavens, *Physics of Thin Films*, Academic Press, (1964)
- D. Keough, *Development of a High Sensitivity Piezoresistance Shock Transducer for the Low Kilobar Range*, DASA #2508, Stanford Research Institute, Menlo Park, California (1970)
- D. Keough and W. Wilkinson (I can't locate the whole paper but it has a lot of usefull information on resistance measurements under shock loading.)
- R.D. Mathis Company, 2840 Gundry Avenue, Long Beach, CA (213) 426-7049. This company makes the tungsten coils for evaporating aluminum films
- M.H. Rice and J.M. Walsh, *Equation of State of Water to 250Kbars*, *J. Chem. Phys.*, Vol. 26, No. 4, (1957)

- Z. Rosenberg and Y. Partom, *Temperature Measurement of Shock Loaded Polymethylmethacrylate with In - Material Nickel Gauges*, J. Appl. Phys., Vol. 52, No. 10, 6133, (1981)
- Z. Rosenberg and Y. Partom, *Direct Measurement of Temperature in Shock - Loaded Polymethylmethacrylate with Very Thin Copper Thermistors*, J. Appl. Phys., Vol. 56, No. 7, 1921, (1984)
- S.A. Sheffield and G.E. Duvall *Response of Liquid Carbon Disulfide to Shock Compression: Equation of State at Normal and High Densities*, J. Chem. Phys. Vol 79, No. 4, 1981, (1983)
- S. Tolczynski, *Summary of Findings Concerning Feasibility of Thermoresistive Temperature Measurements under Uniaxial Stress*, Unpublished, WSUSDL file, (1983?) Tolczynski began this project, and his paper should be read by anyone attempting to continue this work.

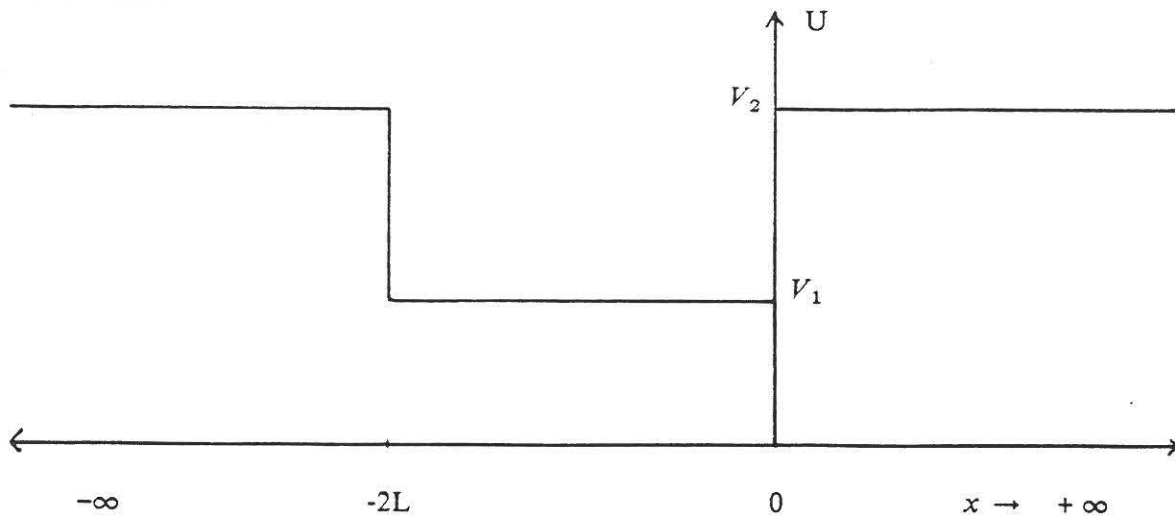
## APPENDIX I

### Solution of the 2 Material 1-D Heat Transfer Problem

The physical problem is as follows: Material 1 is of thickness  $2L$  and extends over a large enough portion of the  $Y-Z$  plane that temperature variations can be considered to occur only in the  $x$  direction. Material 1 is centered at  $x = -L$  and is in thermal contact with material 2 which extends from the boundaries to  $x = \pm\infty$ .



At the time  $t = 0^+$  material 2 has a constant temperature  $V_2$  and material 1 has a constant temperature  $V_1$ . This is thought to correspond to the condition just after the shock wave passes.



Since the problem is symmetric about  $x = -L$  we will solve the heat conduction problem in the region  $-L < x < \infty$ .

### Definitions

$U_1 \equiv$  Temperature in region 1

$U_2 \equiv$  Temperature in region 2

$d_1 \equiv$  Thermal diffusivity in region 1

$d_2 \equiv$  Thermal diffusivity in region 2

$K_1 \equiv$  Thermal conductivity of material 1

$K_2 \equiv$  Thermal conductivity of material 2

$V_1 \equiv$  Initial temperature in region 1

$V_2 \equiv$  Initial temperature in region 2

### The Heat Conduction Equation

$$\frac{\partial^2 U_1}{\partial x^2} - \frac{1}{d_1} \frac{\partial U_1}{\partial t} = 0 \text{ for } -L < x < 0 \text{ and } t > 0.$$

$$\frac{\partial^2 U_2}{\partial x^2} - \frac{1}{d_2} \frac{\partial U_2}{\partial t} = 0 \text{ for } 0 < x < \infty \text{ and } t > 0.$$

### The Boundary Conditions

$$U_1 = U_2 \text{ for } x = 0 \text{ and } t > 0 \tag{1}$$

$$K_1 \frac{\partial U_1}{\partial x} = K_2 \frac{\partial U_2}{\partial x} \text{ for } x = 0 \text{ and } t > 0 \tag{2}$$

$$\frac{\partial U_1}{\partial x} = 0 \text{ at } x = -L \tag{3}$$

### The Initial Conditions

$$U_1 = V_1 \quad \text{for } -L < x < 0 \quad \text{and } t = 0^+$$

$$U_2 = V_2 \quad \text{for } 0 < x < \infty \quad \text{and } t = 0^+$$

### The Algebra

We use a Laplace transform in time. The new variable is  $p$ . Remember that  $L\{\dot{f}(t)\} = pL\{f(t)\} - f(0)$ . For the heat conduction equation we get

$$\frac{d^2 \bar{U}_1}{dx^2} - \frac{p}{d_1} \bar{U}_1 + \frac{V_1}{d_1} = 0$$

$$\frac{d^2 \bar{U}_2}{dx^2} - \frac{p}{d_2} \bar{U}_2 + \frac{V_2}{d_2} = 0$$

We make the substitution  $\frac{p}{d} = q^2$  and get

$$\frac{d^2 \bar{U}_1}{dx^2} - q_1^2 \bar{U}_1 + \frac{V_1}{d_1} = 0$$

$$\frac{d^2 \bar{U}_2}{dx^2} - q_2^2 \bar{U}_2 + \frac{V_2}{d_2} = 0$$

Solutions satisfying these O.D.E.s are

$$\bar{U}_1 = Ae^{q_1 x} + Be^{-q_1 x} + \frac{V_1}{p}$$

$$\bar{U}_2 = Ce^{q_2 x} + De^{-q_2 x} + \frac{V_2}{p}$$

But  $C = 0$  since  $\bar{U}_2$  must be bounded as  $x \rightarrow \infty$ . Applying boundary condition (3) we have

$$\frac{d\bar{U}_1(x = -L)}{dx} = 0$$

$$q_1 [Ae^{q_1 x} - Be^{q_1 x}] = 0 \text{ at } x = -L$$

$$B = Ae^{-2q_1 L}$$

$$\bar{U}_1 = A [e^{q_1 x} + e^{-2q_1 L} e^{-q_1 x}] + \frac{V_1}{p}$$

Applying boundary condition (2) we have

$$K_1 \frac{d\bar{U}_1(x=0)}{dx} = K_2 \frac{d\bar{U}_2(x=0)}{dx}$$

$$K_1 q_1 A [e^{q_1 x} - e^{-2q_1 L} e^{-q_1 x}] = -K_2 q_2 D e^{-q_2 x} \text{ at } x = 0$$

$$\frac{K_1}{\sqrt{d_1}} A [1 - e^{-2q_1 L}] = -\frac{K_2}{\sqrt{d_2}} D$$

$$D = \sigma A (e^{-2q_1 L} - 1)$$

Where  $\sigma = \frac{K_1}{K_2} \sqrt{d_2/d_1}$

$$\bar{U}_1 = A [e^{q_1 x} + e^{-2q_1 L} e^{-q_1 x}] + \frac{V_1}{p}$$

$$\bar{U}_2 = A\sigma [e^{-2q_1 L} - 1] e^{-q_2 x} + \frac{V_2}{p}$$

Applying boundary condition (1),  $\bar{U}_1(x=0) = \bar{U}_2(x=0)$  we get

$$A [1 + e^{-2q_1 L}] + \frac{V_1}{p} = \sigma A [e^{-2q_1 L} - 1] + \frac{V_2}{p}$$

Solving for A we find

$$A = \frac{V_2 - V_1}{p(1 + \sigma)} \frac{1}{1 - \frac{\sigma - 1}{\sigma + 1} e^{-2q_1 L}}$$

If we let  $\frac{\sigma-1}{\sigma+1} = \alpha$  and recall that  $\frac{1}{1-r} = \sum_{n=0}^{\infty} r^n$  for  $r < 1$  then

$$A = \frac{V_2 - V_1}{p(1+\sigma)} \sum_{n=0}^{\infty} \alpha^n e^{-2q_1 n L}$$

For our Laplace transformed temperature  $\bar{U}$  we finally get,

$$\bar{U}_1 = \frac{V_1}{p} + \frac{V_2 - V_1}{p(1+\sigma)} \sum_{n=0}^{\infty} \alpha^n \left[ e^{q_1(z-2nL)} + e^{-q_1(z+2L(n+1))} \right]$$

$$\bar{U}_2 = \frac{V_2}{p} + \frac{V_2 - V_1}{p(1+\sigma)} \sum_{n=0}^{\infty} \alpha^n \left[ e^{-2q_1 L(n+1) - q_1 z} - e^{-2q_1 n L - q_1 z} \right]$$

We look in the tables for an inverse transform and find that with  $q = \sqrt{p/d}$

$$L^{-1} \left[ \frac{1}{p} e^{-qa} \right] = \text{erfc} \left[ \frac{a}{2\sqrt{dt}} \right]$$

Putting  $\bar{U}_2$  in an appropriate form we get

$$\bar{U}_2 = \frac{V_2}{p} + \frac{V_2 - V_1}{p(1+\sigma)} \sum_{n=0}^{\infty} \alpha^n \left\{ e^{-\sqrt{p} \left| \frac{2L(n+1)}{\sqrt{d_1}} + \frac{z}{\sqrt{d_2}} \right|} - e^{-\sqrt{p} \left| \frac{2nL}{\sqrt{d_1}} + \frac{z}{\sqrt{d_2}} \right|} \right\}$$

We get the solutions by taking the inverse transform

$$\bar{U}_1(x,t) = V_1 + \frac{V_2 - V_1}{1 + \sigma} \sum_{n=0}^{\infty} \alpha^n \left\{ \operatorname{erfc} \left( \frac{2nl - x}{2\sqrt{d_1 t}} \right) + \operatorname{erfc} \left( \frac{x + 2L(n+1)}{2\sqrt{d_1 t}} \right) \right\}$$

$$\bar{U}_2(x,t) = V_2 + \frac{V_2 - V_1}{1 + \sigma} \sum_{n=0}^{\infty} \alpha^n \left\{ \operatorname{erfc} \left[ \frac{1}{2\sqrt{t}} \left[ \frac{2L(n+1)}{\sqrt{d_1}} + \frac{x}{\sqrt{d_2}} \right] \right] - \operatorname{erfc} \left[ \frac{1}{2\sqrt{t}} \left[ \frac{2nL}{\sqrt{d_1}} + \frac{x}{\sqrt{d_2}} \right] \right] \right\}$$

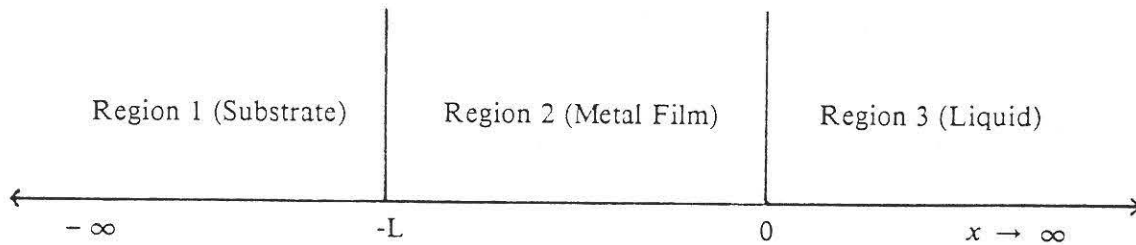
The methods used here are outlined in Carslaw and Jaeger chapter 12 (especially section 12.4).

The Laplace Transform pairs are from appendix V. The equation used to evaluate the erfc in the computer program is found in appendix II (4).

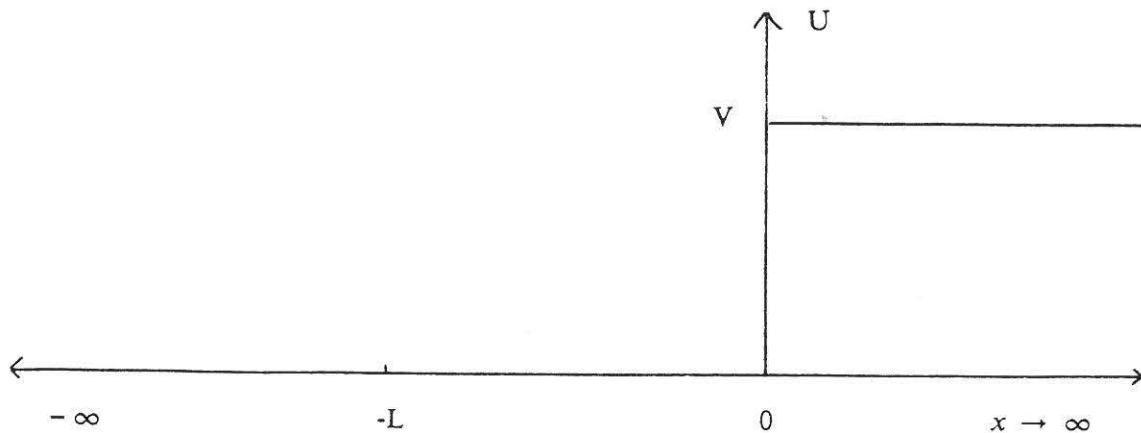
## APPENDIX II

### Solution of the 3 Material 1-D Heat Conduction Problem

This is intended to simulate the heat transfer problem for a thin metal film which is in thermal contact with a shocked liquid and a substrate. Material 1 is the substrate and extends from  $x = -L$  to  $x = -\infty$ . Material 2 is the metal film. It extends from  $-L$  to  $0$ . Material 3 is the liquid. It extends from  $0$  to  $\infty$ .



At time  $t = 0^+$  Material 3 has temperature  $V$  and materials 1 and 2 have temperature 0. This can be scaled later by changing  $V$  to the temperature difference and adding the initial temperature to each of the solutions. These initial conditions are thought to simulate the condition just after the shock wave passes the gauge.



### The Definitions

See Appendix I definitions.

### The Heat Conduction Equations

$$\frac{\partial^2 U_1}{\partial x^2} - \frac{1}{d_1} \frac{\partial U_1}{\partial t} = 0 \quad \text{for } -\infty < x < -L \text{ and } t > 0.$$

$$\frac{\partial^2 U_2}{\partial x^2} - \frac{1}{d_2} \frac{\partial U_2}{\partial t} = 0 \quad \text{for } -L < x < 0 \text{ and } t > 0.$$

$$\frac{\partial^2 U_3}{\partial x^2} - \frac{1}{d_3} \frac{\partial U_3}{\partial t} = 0 \quad \text{for } 0 < x < \infty \text{ and } t > 0.$$

### The Boundary Conditions

$$U_1(-L, t) = U_2(-L, t) \tag{1}$$

$$K_1 \frac{\partial U_1(-L, t)}{\partial x} = K_2 \frac{\partial U_2(-L, t)}{\partial x} \tag{2}$$

$$U_2(0, t) = U_3(0, t) \tag{3}$$

$$K_2 \frac{\partial U_2(0, t)}{\partial x} = K_3 \frac{\partial U_3(0, t)}{\partial x} \tag{4}$$

### The Initial Conditions

$$U_1(x, 0^+) = 0$$

$$U_2(x, 0^+) = 0$$

$$U_3(x, 0^+) = V$$

### The Algebra

As in Appendix I we take a Laplace transform to get the O.D.E.s

$$\frac{d^2 \bar{U}_1}{dx^2} - q_1^2 \bar{U}_1 = 0$$

$$\frac{d^2 \bar{U}_2}{dx^2} - q_2^2 \bar{U}_2 = 0$$

$$\frac{d^2 \bar{U}_3}{dx^2} - q_3^2 \bar{U}_3 + \frac{V}{d_3} = 0$$

Solutions satisfying these equations are

$$\bar{U}_1 = A e^{q_1 x}$$

$$\bar{U}_2 = B e^{q_2 x} + C e^{-q_2 x}$$

$$\bar{U}_3 = D e^{-q_3 x} + \frac{V}{p}$$

Applying boundary condition (2) we have

$$K_1 \frac{d\bar{U}_1(-L)}{dx} = K_2 \frac{d\bar{U}_2(-L)}{dx}$$

$$K_1 q_1 A e^{-q_1 L} = K_2 q_2 \left( B e^{-q_2 L} - C e^{q_2 L} \right)$$

$$A = \frac{K_2}{K_1} \sqrt{d_1/d_2} \left( B e^{-q_2 L} - C e^{q_2 L} e^{q_1 L} \right)$$

And we let  $\frac{K_2}{K_1} \sqrt{d_1/d_2} = \sigma_1$

Applying boundary condition (1)  $\bar{U}_1(-L) = \bar{U}_2(-L)$  we have

$$\sigma_1 \left( B e^{-q_1 L} - C e^{q_1 L} \right) e^{q_1 L} e^{-q_1 L} = B e^{-q_1 L} + C e^{q_1 L}$$

Collecting terms and solving for C we get

$$C = B \frac{\sigma_1 - 1}{\sigma_1 + 1} e^{-2q_1 L} = B \alpha_1 e^{-2q_1 L}$$

Upon back substitution we get

$$\bar{U}_1 = B \sigma_1 \left( 1 - \alpha_1 \right) e^{-q_1 L} e^{q_1 (L+x)}$$

$$\bar{U}_2 = B \left( e^{q_1 x} + \alpha_1 e^{-q_1 (2L+x)} \right)$$

We now apply boundary condition (4)  $K_2 \frac{d\bar{U}_2(0)}{dx} = K_3 \frac{d\bar{U}_3(0)}{dx}$ .

$$K_2 q_2 B \left( \alpha_1 e^{-2q_1 L} - 1 \right) = K_3 q_3 D$$

Solving for D we get

$$D = B \frac{K_2}{K_3} \sqrt{d_3/d_2} \left( \alpha_1 e^{-2q_1 L} - 1 \right) = B \sigma_2 \left( \alpha_1 e^{-2q_1 L} - 1 \right)$$

Finally we apply boundary condition (3)  $\bar{U}_2(x=0) = \bar{U}_3(x=0)$

$$B \left( 1 + \alpha_1 e^{-2q_1 L} \right) = B \sigma_2 \left( \alpha_1 e^{-2q_1 L} - 1 \right) + \frac{V}{p}$$

Collecting terms we get

$$B \left[ 1 + \sigma_2 + \alpha_1(1-\sigma_2)e^{-2q_1L} \right] = \frac{V}{p}$$

Dividing both sides by  $1+\sigma_2$

$$B \left[ 1 - \alpha_1 \frac{\sigma_2-1}{\sigma_2+1} e^{-2q_1L} \right] = \frac{V}{p(1+\sigma_2)}$$

We set  $\frac{\sigma_2-1}{\sigma_2+1} = \alpha_2$  and solve for B.

$$B = \frac{V}{p(1+\sigma_2)} \frac{1}{1-\alpha_1\alpha_2 e^{-2q_1L}}$$

Rewriting this as a geometric series we have

$$B = \frac{V}{p(1+\sigma_2)} \sum_{n=0}^{\infty} (\alpha_1\alpha_2)^n e^{-2nLq_1}$$

Substituting B back into the Laplace transformed temperatures we get

$$\bar{U}_1 = \frac{\sigma_1(1-\alpha_1)V}{p(1+\sigma_2)} \sum_{n=0}^{\infty} (\alpha_1\alpha_2)^n e^{[-q_1L(2n+1)+q_1(L+x)]}$$

$$\bar{U}_2 = \frac{V}{P(\sigma_2+1)} \sum_{n=0}^{\infty} (\alpha_1\alpha_2)^n \left[ e^{-q_1(2nL-x)} + \alpha_1 e^{-q_1(2L(n+1)+x)} \right]$$

$$\bar{U}_3 = \frac{V}{p} + \frac{\sigma_2 V}{P(\sigma_2+1)} \sum_{n=0}^{\infty} (\alpha_1\alpha_2)^n \left[ \alpha_1 e^{-q_1 2L(n+1)-q_1 x} - e^{-q_1 2nL-q_1 x} \right]$$

Recalling that  $V = V_3 - V_1$  and that  $V_2 = V_1$  and then inverting the transform we get the temperatures in the three regions.

$$U_1(x,t) = V_1 + \frac{(V_3 - V_1)(1 - \alpha_1)}{\sigma_2 + 1} \sum_{n=0}^{\infty} (\alpha_1 \alpha_2)^n \operatorname{erfc} \left[ \frac{1}{2\sqrt{t}} \left( \frac{L(2n+1)}{\sqrt{d_2}} - \frac{L+x}{\sqrt{d_1}} \right) \right]$$

$$U_2(x,t) = V_1 + \frac{V_3 - V_1}{\sigma_2 + 1} \sum_{n=0}^{\infty} (\alpha_1 \alpha_2)^n \left[ \operatorname{erfc} \left( \frac{2nL - x}{2\sqrt{d_2 t}} \right) + \alpha_1 \operatorname{erfc} \left( \frac{2L(n+1) + x}{2\sqrt{d_2 t}} \right) \right]$$

$$U_3(x,t) = V_3 + \frac{\sigma_2 (V_3 - V_1)}{\sigma_2 + 1} \sum_{n=0}^{\infty} (\alpha_1 \alpha_2)^n \left\{ \alpha_1 \operatorname{erfc} \left[ \frac{1}{2\sqrt{t}} \left( \frac{2L(n+1)}{\sqrt{d_2}} + \frac{x}{\sqrt{d_3}} \right) \right] - \operatorname{erfc} \left[ \frac{1}{2\sqrt{t}} \left( \frac{2nL}{\sqrt{d_2}} + \frac{x}{\sqrt{d_3}} \right) \right] \right\}$$

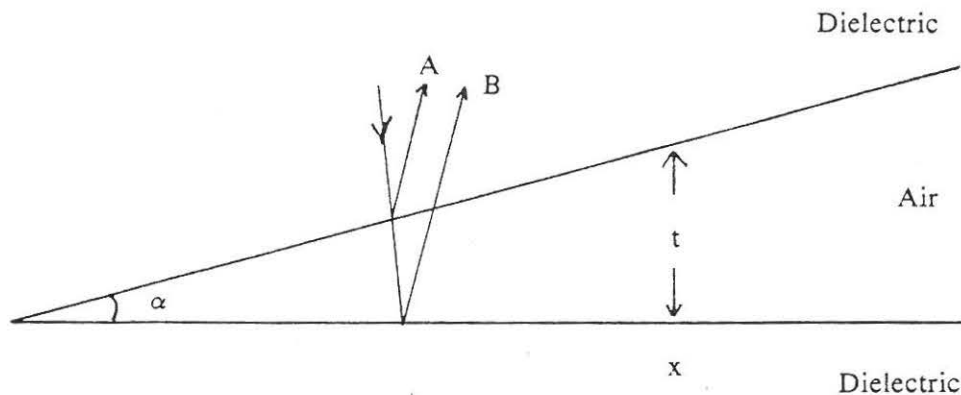
As is also true for the solution given in appendix I this solution is almost meaningless without a computer evaluation and graphics to tell you what it means. The methods I have used here are again found in Carslaw and Jaeger Chapter 12.

### APPENDIX III

#### Thickness Measurements for Thin Films

Although there are a number of methods for measuring the thickness of thin films, Tolansky's method is easily understood and easily set up. The method is outlined in many books on thin films, as well as many books on optics. (See for an example chapter 7 of Born and Wolf especially section 7.6 ) The method is based on simple light interference effects.

Suppose we have a wedge shaped layer of air between two dielectric plates. A monochromatic light source is shining on it.



Ray B has a phase change of  $\pi$  on reflection, but ray A has no phase change. We expect to see dark fringes when A and B are  $\pi$  out of phase and bright fringes when they are in phase. If  $t$  is the thickness of the gap at any point then we will get dark fringes when

$$2t = 0, \lambda, 2\lambda, \dots, m\lambda.$$

We will get bright fringes when

$$2t = \frac{\lambda}{2}, \frac{3\lambda}{2}, \frac{5\lambda}{2}, \dots$$

If  $x$  is the distance along the wedge and  $\alpha$  the angle of the wedge

$$t = x \tan \alpha \text{ or } x = \frac{t}{\tan \alpha}.$$

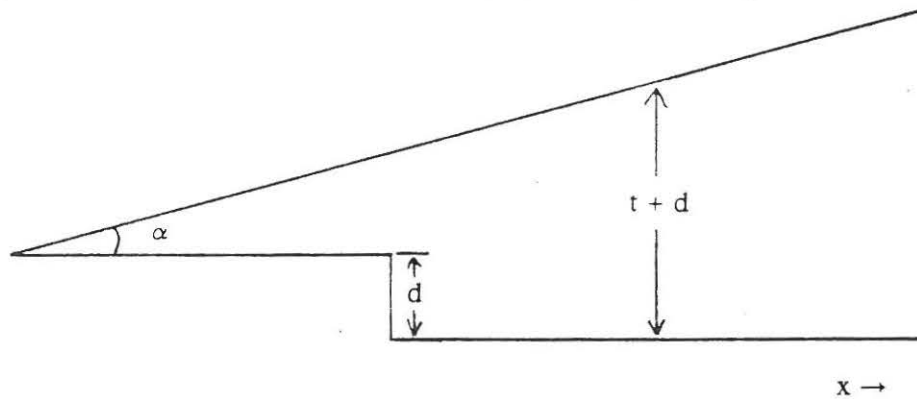
For dark fringes  $t = \frac{m\lambda}{2}$  and the location of the fringe will be at  $x_m$  where

$$x_m = \frac{tm}{\tan \alpha} = \frac{m\lambda}{2 \tan \alpha}$$

Note that all fringes are equally spaced a distance  $L$  apart where

$$L = \frac{\lambda}{2 \tan \alpha}$$

Note also that for small angles the fringes will be widely spaced;  $L \rightarrow \infty$  as  $\alpha \rightarrow 0$ . Now suppose there is a step of thickness  $d$  in the material of the lower half of the wedge.



The condition for a dark fringe is now

$$2(t + d) = m\lambda$$

If  $\hat{x}$  is the new location of the fringe

$$\hat{x} \tan \alpha + d = \frac{m\lambda}{2}, \text{ and}$$

$$\hat{x} = \frac{\frac{m\lambda}{2} - d}{\tan \alpha}$$

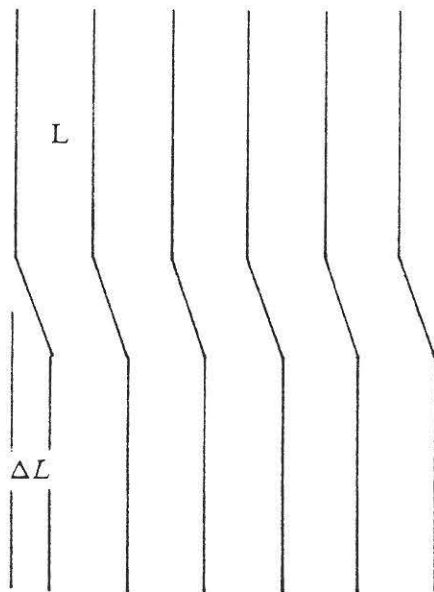
If we define the fringe shift as  $\Delta L = x - \hat{x}$

$$\Delta L = \frac{m\lambda}{2 \tan \alpha} - \frac{m\lambda}{2 \tan \alpha} + \frac{d}{\tan \alpha} = \frac{d}{\tan \alpha}$$

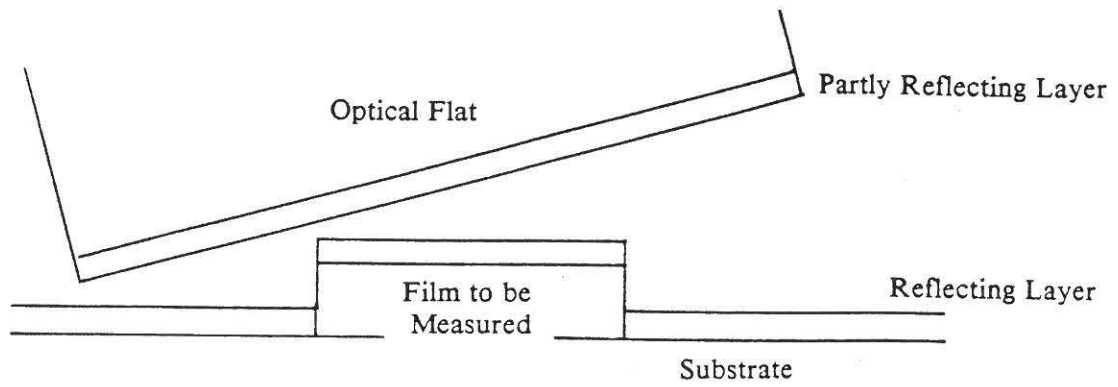
$$\frac{\Delta L}{L} = \frac{\frac{d}{\tan \alpha}}{\frac{\lambda}{2 \tan \alpha}}, \text{ which we get}$$

$$d = \frac{\lambda}{2} \frac{\Delta L}{L}, \text{ which is the step thickness.}$$

If we can arrange a system such that the fringes are running in one direction and the step is in another direction we will get a fringe pattern like the one below.



For measuring the thickness of deposited films the experimental set up is as in the picture below.



The reflecting layer on the substrate and the partially reflecting layer on the optical flat are necessary for good contrast between the dark and bright fringes. The fringes are generally photographed under a sodium light (5893 angstroms) using a close up lens. The measurements of  $\Delta L$  and  $L$  are then made from the print. This method only works well for films less than half a wavelength thick.

## APPENDIX IV

### Substrate Cleaning and Vapor Deposition Recipes

#### Substrate Cleaning

The following procedure generally works well for glass like substrates such as sapphire or fused silica.

- (1) Remove any coarse stuff using acetone and a Kimwipe. Rinse with distilled  $H_2O$  and dry with an EFFA duster.
- (2) Swab the substrate with pure nitric acid using a Q-tip. This will remove most oils. Rinse with distilled  $H_2O$  and dry with an EFFA duster.
- (3) Swab the surface with 25% HF using a Q-tip. This provides a light etch to the surface. Do not rinse the surface too long in the HF or it will become badly pitted. Rinse off the HF after about 30 seconds using distilled  $H_2O$  and dry the surface with an EFFA duster.
- (4) After the last rinse and dry put the substrate directly into the vacuum evaporator. Be very careful to avoid putting fingerprints on it.

## Vapor Deposition

I generally use the following procedure:

- (1) Be clean. Avoid getting body oils (fingerprints) on the evaporant, the crucible, or the target. Use only clean materials and crucibles.
- (2) Vacuum should be less than  $10^{-5}$  torr but need not be lower than  $10^{-6}$  torr.
- (3) The substrate (target) should be more than 4" away from the evaporant source. I use 6-8" for aluminum and about 4" for copper.
- (4) To evaporate aluminum I use an R.D. Mathis F2-3x.025 W tungsten filament loaded with 2-4 65mg clips of aluminum. Aluminum is best "flashed" or deposited very rapidly. With this filament use about 40 amps until the aluminum clips melt. Then increase the current to 50 amps. When all the aluminum has evaporated (this usually takes less than a minute) the current will drop below 50 amps. If the purity of the film is important, use a fresh tungsten filament each time. The aluminum can alloy to the tungsten resulting in tungsten impurities in the films. Since each filament costs less than 2 dollars don't worry about expense.
- (5) To evaporate copper use an aluminum oxide coated crucible. Most of the copper sample we have is not high purity and must further be shaped by hand before it will go in the crucible. Because it will be dirty always use a shutter. With the shutter closed, heat the copper till it melts, using about 30 amps of current. Keep the shutter closed till all the slag floating on top of the molten copper has burned off. Open the shutter and deposit to the desired thickness. For most purposes, when you can't see through the bell jar it is thick enough.

- (6) **Tape Test:** To test the adhesion of your film press a piece of masking tape on the film and then peel it off. Aluminum films very often pass this test. Copper films very often fail it.
- (7) The adhesion of aluminum films can often be enhanced by baking them at 300 - 500 C under vaccum or in a nitrogen or argon atmosphere.

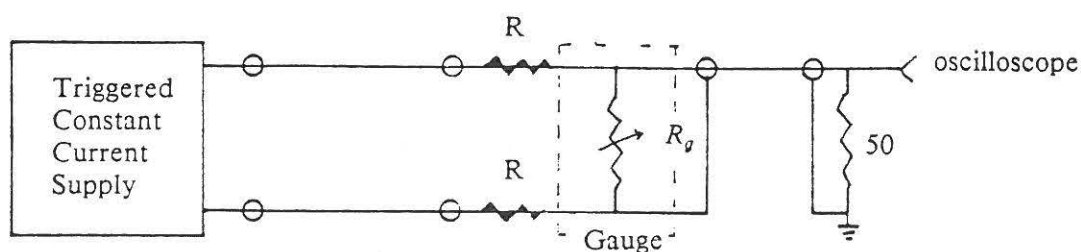
#### Miscelaneous

A good refererence for evaporant sources is the paper by Archibald and Parent. The address for the maker of the tungsten fillaments is listed in the references under R.D. Mathis Company.

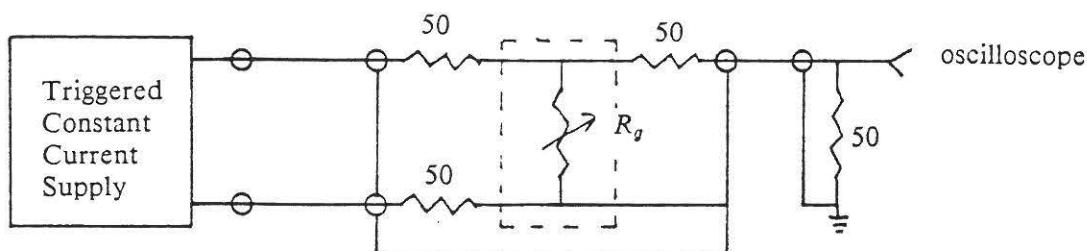
## APPENDIX V

### Circuits for High Speed Time Resolved Four Terminal Resistance Measurements

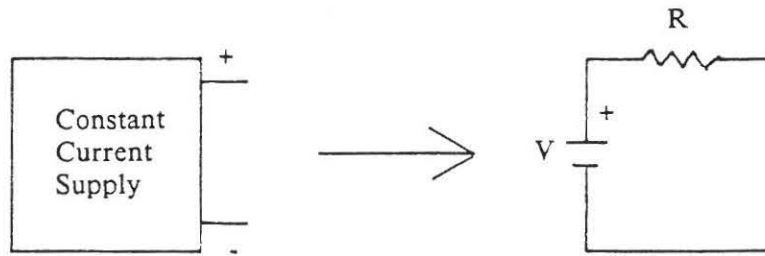
The simplest form of recording system consists of four parts; A constant current power supply, a gauge circuit, a recording circuit, and recording instruments such as oscilloscopes.



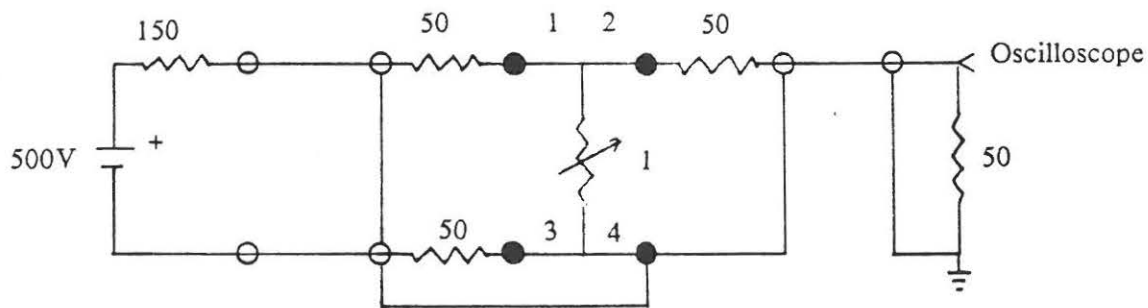
The above circuit is of the simplest type. The resistors "R" are for the purpose of current limiting only. While it has been used with success in the manganin gauge research in our lab, high frequency circuit principles have not been applied. The cable terminations are not matched to the line etc. Since all cables used in our lab are of the 50 ohm impedance variety, 50 ohm terminations should be used on all cables. A much improved circuit (from Keough and Wilkinson) is shown below. Another important reference is Keough's 1970 paper. Any additional current limiting should be done with 50 ohm attenuators at the power supply. This circuit gives very smooth, fast rising signals.



In order to more fully understand the behaviour of the system we need to replace the constant current power supply with its equivalent circuit model. There is, of course, no such thing as a constant current power supply. Most can be modeled as a voltage source in series with a large current limiting resistance.

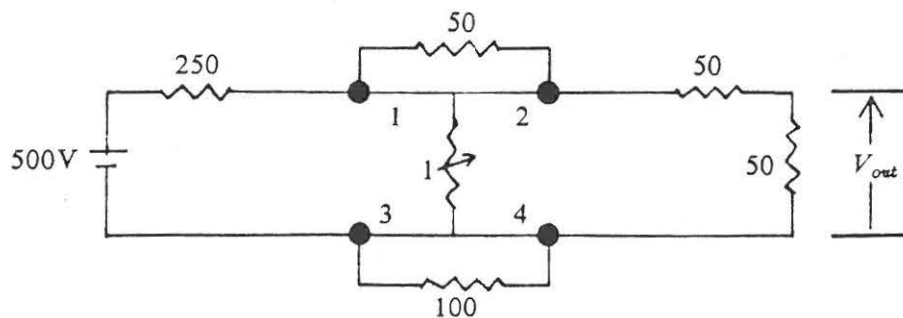


For my experiments the supply voltage was 500 volts and the series resistance 150 ohms. If we neglect cable capacitances the circuit shown below describes the recording system quite well.



Apparently for the breakage of the leads (labelled as 1,2,3,4) the cables, acting as charged capacitors will discharge through the 50 ohm oscilloscope resistance. This could easily be the cause of the large fast rising voltage seen in some of the experiments.

To test for lead breakage shunt resistances were placed across the leads. Breakage of a lead or combination of leads would result in a particular voltage signature at the oscilloscope. The simplified equivalent "Lead Breakage Circuit" is shown below.



The following table gives the output voltage for breakage of various leads.

# of Lead(s) Broken	Voltage at Scope
none	.986
1	.822
2	.660
3	.705
4	.496
1,2	62.5
1,3	.612
1,4	.413
2,3	.472
2,4	.397
3,4	55.6
any 3 or 4	50.0
Gauge only	71.4

Because of the circular symmetry of the gauge system the most common lead breakages would be; none, all four leads broken, or gauge only broken. The recording system must now include at least two oscilloscopes; one for the regular signal assuming the gauge survives, and one set at about 100 volts full scale for the high voltages.

## INTERNAL REPORTS - 1988

1. Z.P. Tang, "Data Reduction of the Half-Inch Shorted Quartz Gauge Record Using the Code Interp", Internal Report 88-01, November, 1987.
2. Z.P. Tang, "Numerical Simulations of Wave Propagation in CdS/BAMO:THF Composite", Internal Report 88-02, November, 1987.
3. G.E. Duvall, "Interpretation of Densitometer Records", Internal Report 88-03, February, 1988.
4. S. Sharma, "Optical Spectrum of Ruby: Application to Shock Deformation", Internal Report 88-04, January, 1988.
5. P.D. Horn, "Crystallographic Directions and Elastic Constants in  $\text{Al}_2\text{O}_3$ ", Internal Report 88-05, February, 1988.
6. P.D. Horn, "Feasibility of Measuring Polarized Absorption Spectra of Ruby", Internal Report 88-06, June, 1988.
7. P. Horn, "Data Reduction in Ruby Luminescence Experiments", Internal Report 88-07, June, 1988.
8. G.E. Duvall, "Program for Fitting P.V. Data to a Murnaghan Equation", Internal Report 88-08, July, 1988.